2018

# Structural Identification and Kinetic Analysis of the in Vitro Products Formed by Reaction of Bisphenol A-3,4-quinone with N-Acetylcysteine and Glutathione

Douglas E. Stack
*University of Nebraska at Omaha*, dstack@unomaha.edu

John A. Conrad
*University of Nebraska at Omaha*, jaconrad@unomaha.edu

Bejan Mahmud
*University of Nebraska Omaha*, bmahmud@unomaha.edu



## Recommended Citation

Structural Identification and Kinetic Analysis of the in Vitro Products Formed by Reaction of Bisphenol A-3,4-quinone with N-Acetylcysteine and Glutathione Douglas E. Stack, John A. Conrad, and Bejan Mahmud Chemical Research in Toxicology Article ASAP DOI: 10.1021/acs.chemrestox.7b00239

Chemical Research in Toxicology

ACS AuthorChoice

Article

Cite This: Chem. Res. Toxicol. XXXX, XXX, XXX−XXX

pubs.acs.org/crt

# Structural Identification and Kinetic Analysis of the *in Vitro* Products Formed by Reaction of Bisphenol A-3,4-quinone with *N*-Acetylcysteine and Glutathione

Douglas E. Stack,* John A. Conrad, and Bejan Mahmud

Department of Chemistry, University of Nebraska at Omaha, 6001 Dodge Street, Durham Science Center, Omaha, Nebraska 68182, United States

Supporting Information

**ABSTRACT:** Bisphenol A (BPA) has received considerable attention as an endocrine disrupting chemical and a possible substrate for genotoxic metabolites. BPA metabolism leads to formation of electrophilic *o*-quinones cable of binding to DNA and other endogenous nucleophiles. We have structurally identified the products resulting from the reaction of bisphenol A-3,4-quinone (BPAQ) with *N*-acetylcysteine (NAC) and glutathione (GSH). The major and minor isomers are both the result of 1,6-conjugate addition and are produced almost instantly in high yield. Reactions using 1.3 equiv of GSH showed the presence of a bis-glutathionyl adduct which was not observed using higher GSH concentration relative to BPAQ. NAC reactions with BPAQ showed no bis-*N*-acetylcysteinyl adducts. Stopped-flow kinetic analysis reveals the 1,6-conjugate additions to be reversible with a forward free energy of activation of 9.2 and 7.8 kcal/mol for the NAC and GSH reactions, respectively. The bimolecular forward rate constant at 19.4 °C was approximately three time faster for GSH compared to NAC, 1547 vs 496 $M^{-1}$ $s^{-1}$. The free energy of activation for the reverse reactions were similar, 11.7 and 11.2 kcal/mol for NAC and GSH, respectively. We plan to use this model system to further explore the mechanism of adduct formation between sulfur nucleophiles and *o*-quinones and the resulting chemical properties of both NAC and GSH adducts.

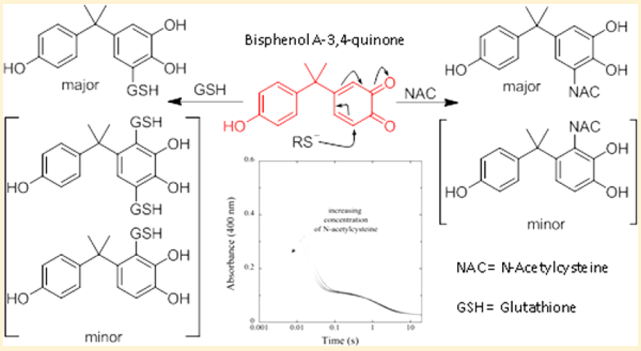


## INTRODUCTION

Bisphenol A (BPA) is a widely used industrial chemical prominent in the manufacture of plastics and epoxy resins.[1] BPA and its metabolites can act as estrogen mimics and are classified as endocrine disrupting chemicals.[2] Evidence for genotoxic effects *in vitro* have been revealed in studies involving mouse lymphoma,[3] MCF-7[4] and CHO-K1[5] cells. *In vivo* studies showed structural changes in bone marrow cells of mice.[6]

The major metabolites of BPA include glucuronic acid conjugates and catechols.[7] Catechols can undergo further oxidation to *o*-quinones (Scheme 1), known genotoxic compounds cable of binding to the nucleosides of DNA. The mono-*o*-quinone of BPA, BPA-3,4-quinone (BPAQ), reacts with deoxyguanosine via 1,4-conugate addition.[8,9] BPAQ-DNA adducts have been detected *in vitro* and *in vivo* with either BPAQ exposure or metabolically activated BPA.[10,11] BPAQ chemistry has shown to be analogous to estrogen *o*-quinones, known genotoxic metabolites.[12] Glutathione (GSH) is a prominent *o*-quinone scavenger. Several studies have shown the production BPAQ-GSH adducts *in vitro* as analyzed by LC/MS[9,13] which confirmed the presence of catechol-GSH products but did not indicate the regiochemistry of the conjugate addition, namely 1,4- versus 1,6-addition. Soft sulfur nucleophiles show a preference for 1,6-addition with various *o*-quinones, but 1,4-addition products are also observed.[14,15]

Recently we have developed a large-scale synthetic approach to the BPA metabolites, BPAQ, the di-*o*-quinone of BPA, the monocatechol of BPA, and the dicatechol of BPA.[16] With this

**Scheme 1. Metabolism of BPA and Conjugation with Sulfur Nucleophiles**

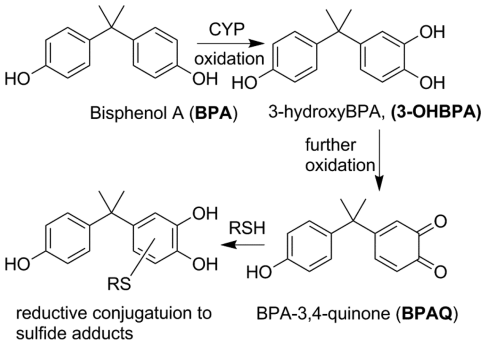


Received: August 25, 2017
Published: December 27, 2017




DOI: 10.1021/acs.chemrestox.7b00239
Chem. Res. Toxicol. XXXX, XXX, XXX−XXX

new synthetic technique at hand, we sought to determine the major product(s) when BPAQ reacts with NAC and GSH. Scheme 2 shows the three possible conjugate addition products

**Scheme 2. Possible Isomers from the Reaction of BPAQ with Sulfur Nucleophiles**[a]

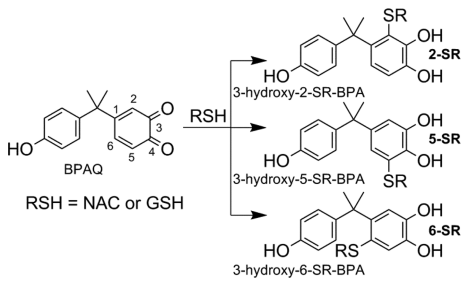


[a]**2-SR** and **5-SR** are products of 1,6-addition, while **6-SR** would result from 1,4-addition.

when BPAQ reacts with these sulfur nucleophiles. Products **2-SR** and **5-SR** are the result of 1,6-addition with respect to BPAQ C4 and C3 carbonyls, respectively. Adduct **6-SR** would result from 1,4-addition with respect to BPAQ C4 carbonyl.

BPAQ is a relatively stable *o*-quinone with a deep red color in organic solvents. We recognized that the stability of BPAQ combined with its chromophore properties would make kinetic analysis of the conjugate addition possible. Conjugate addition of sulfur nucleophiles to certain quinones has shown reversible characteristics indicating that sulfur detoxification may lead to other metabolic processes.[17−19] Second-order rate constants for both NAC and GSH conjugate addition to various Michael acceptors have been measured and shown to be a function of both steric and electronic factors of the electrophile in addition to the p$K_a$ of the thiol nucleophile.[20−22]

Herein we described the synthesis and full structural characterization of the NAC and GSH adducts of BPAQ. In addition, the measurement of second-order rate constants using stopped-flow techniques and the resulting thermodynamic parameters are presented to establish a better understanding of the reversible mechanism involved with thiol Michael additions to *o*-quinones.

## EXPERIMENTAL PROCEDURES

**Chemicals and Reagents.** 2-Iodoxybenzoic acid (IBX) was synthesized by the method of Frigerio.[23] **Caution:** *IBX is explosive under impact if heated to more than 200 °C.* BPAQ was made by IBX oxidation of BPA[16] with modifications to product isolation (see below). Deuterated NMR solvents were purchased from Cambridge Isotope (Andover, MA). All other chemicals and solvents were purchased from Fisher Scientific Co. (Fair Lawn, NJ) or Aldrich Chemical Co. (Milwaukee, WI) and used as received.

**Instrumentation.** NMR analysis was obtained on a Bruker 400 MHz Avance III spectrometer (Bruker, Billerica, MA, USA). HPLC was conducted on a Waters 2690 Separations Module (Waters Corp. Milford, MA, USA) equipped with a Waters 2487 dual $\lambda$ absorbance detector using solvent gradients consisting of acetonitrile and 0.5% aqueous formic acid on a YMC, ODS-AQ C18 analytical column (5 $\mu$m, 120 Å, 250 mm × 4.5 mm, YMC America, Allentown, PA, USA). Flash column purification of compounds was performed on a Biotage Isoler One (Biotage, Charlotte, NC) automated system using Biotage KP-Shere 30 g and SNAP Ultra HP 12 g C18 columns. Stopped-flow analysis was done on TgK Scientific, KinetAsyst system (TgK Scientific, Bradford-on-Avon, UK). Reaction traces were fit to a sum of three exponentials using KaleidaGraph (Synergy Software, Reading, PA, USA) . HRMS analysis was conducted at the Nebraska Center for Mass Spectrometry (University of Nebraska-Lincoln, Lincoln, NE). Elemental analysis was obtained at MHW Laboratories (Phoenix, AZ).

**Synthesis of 3-Hydroxy-5-NAC-BPA and 3- Hydroxy -2-NAC-BPA.** BPA (0.250 g, 1.10 mmol) was dissolved in 50 mL of a solvent mixture consisting of 3:2 $CHCl_3$:$CH_3OH$ in a 100 mL round-bottom, equipped with a magnetic stir bar and brought to −15 °C. To this solution was added IBX 0.337 g (1.20 mmol) causing the solution to turn deep red after approximately 15 min. The mixture was stirred at −15 °C for 12 h and transferred to a 250 mL separatory funnel, and the chloroform layer was washed 6 × 50 mL with a 0.1 M phosphate buffer, pH 6.0, to remove the *o*-iodobenzoic acid byproduct. The chloroform solvent was removed via rotovap, and the crude was placed in 50 mL of methanol. HPLC analysis of the crude methanol solution showed >95% BPAQ which was used without further purification. *N*-Acetylcysteine (235 mg, 1.43 mmol) was dissolved in 5 mL of 0.1 M phosphate buffer, pH 6.2, and added in one portion to the BPAQ solution. The mixture decolorized instantly from bright red to a light yellow color. The mixture was stirred an additional 10 min at rt, an HPLC sample was removed, and all solvents removed via rotovap. The crude mixture was dissolved in 1−2 mL of methanol and placed on a preconditioned Biotage 30 g C18 flash column (see Figure S1 for flash chromatograph with solvent gradient). Each collection tube was analyzed by HPLC on an analytical column, and three fractions were collected: one containing analytical grade **5-NAC**, a middle fraction containing a mixture of **5-NAC** and **2-NAC**, and fraction containing analytical grade **2-NAC**. The middle fraction was subject to a second separation using a 12 g C18 SNAP Ultra column, solvents were removed, and solids dried overnight under high vacuum at 50 °C to afford a total of 319 mg (81%) of 3-hydroxy-5-NAC-BPA and 27 mg (7%) of 3-hydroxy-2-NAC-BPA.

*3-Hydroxy-5-NAC-BPA.* Needle white solid; $^1$H NMR (DMSO-$d_6$, 400 MHz): $\delta$ 1.52 (s, 6H), 1.84 (s, 3H), 2.95 (dd, $J$ = 13.4 and 9.2 Hz, 1H), 3.23 (dd, $J$ = 13.4 and 4.7 Hz, 1H), 4.28 (m, 1H), 6.43 (d, $J$ = 2.2 Hz, 1H), 6.65 (d, $J$ = 8.7 Hz, 2H), 6.68 (d, $J$ = 2.2 Hz, 1H), 7.00 (d, $J$ = 6.7 Hz,2H) 8.24 (d, $J$ = 8.0 Hz), 9.18 (bs, phenolic OH partially exchanged), 12.67 (very bs, carboxylate OH). For $^1$H spectrum with structure assignment see Supporting Information, p S-4. $^{13}$C NMR (DMSO-$d_6$, 100 MHz): $\delta$ 22.39, 30.71, 30.73, 33.76, 41.14, 51.70, 113.65, 114.59, 118.72, 119.69, 127.30, 140.81, 141.90, 142.17, 144.60, 154.95, 169.27, 172.27. For $^{13}$C spectrum with structure assignment see S-5. Anal. calcd for $C_{20}H_{23}NO_6S$: C, 59.25; H, 5.72; N, 3.45; S, 7.91. Found: C, 59.45; H, 5.84; N, 3.30; S, 8.18.

*3-Hydroxy-2-NAC-BPA.* White solid; $^1$H NMR (DMSO-$d_6$, 400 MHz): $\delta$ 1.58 (s, 3H), 1.62 (s, 3H), 1.83 (s, 3H), 2.51(m, 1H, peak obscured by residual DMSO), 2.69 (dd, $J$ = 12.5 and 4.7 Hz. 1H), 4.04 (m, 1H), 6.57 (d, $J$ = 8.5 Hz, 1H), 6.76 (d, $J$ = 8.9 Hz, 1H), 6.79 (d, $J$ = 8.5 Hz, 1H), 6.86 (d, $J$ = 8.9 Hz, 1H), 7.98 (d, $J$ = 7.8 Hz), 9.17 (bs, 3H phenolic OH partially exchanged). For $^1$H spectrum with structure assignment see S-10. $^{13}$C NMR (DMSO-$d_6$, 100 MHz): $\delta$ 22.34, 30.96, 42.80, 52.05, 114.03, 114.44, 116.73, 142.12, 143.05, 143.74, 147.69, 154.26,169.16, 172.13. For $^{13}$C spectrum with structure assignment see S-11. HRMS (ESI+); calcd for $C_{20}H_{23}NO_6S[M + H]^+$: 406.1246; found: 406.1253.

**Synthesis of 3-Hydroxy-2,5-diGSH-BPA, 3- Hydroxy-5-GSH-BPA, and 3- Hydroxy-2-GSH-BPA.** A 1.10 mmol solution of BPAQ was made as above except after workup, BPAQ was dissolved in 50 mL of 50:50 methanol:water solvent system. GSH (572 mg, 1.43 mmol) was dissolved in 5 mL of 0.1 M phosphate buffer, pH 6.2, and added in one portion to the BPAQ solution. The mixture was stirred at rt for 15 min, and solvents removed via rotovap. The crude solid was dissolved in 50 mL of water and extracted 3 × 25 mL with ethyl acetate to remove the 3-hydroxy-BPA reduction byproduct. The ethyl acetate extract was dried over magnesium sulfate, and solvent removed via rotvap. The aqueous phase was then reduced to 2 mL via rotovap and placed on a preconditioned Biotage 30 g C18 SANP Ultra flash column (see Figure S2 for flash chromatograph with solvent gradient). Each collection tube was analyzed by HPLC on an analytical column, and four fractions containing pure **2,5-diGSH**, a mixture of **2,5-diGSH** and **5-GSH**, pure **5-GSH**, and pure **2-GSH** were collected.


DOI: 10.1021/acs.chemrestox.7b00239
Chem. Res. Toxicol. XXXX, XXX, XXX−XXX

The fraction containing the **2,5-GSH/5-GSH** mixture was subjected to a second separation using a Biotage 30 g C18 SANP Ultra flash column, solvents were removed, and solids dried overnight under high vacuum at 50 °C to afford a total of 151 mg of 3-hydroxy-2,5-diGSH-BPA (17%), 212 mg of 3-hydroxy-5-GSH-BPA (36%), 43 mg of 3-hydoxy-2-GSH (7%), and 81 mg of 3-hydroxyBPA (32%)

*3-Hydroxy-5-GSH-BPA*. Off-white solid; $^1$H NMR (DMSO-$d_6$, 400 MHz): $\delta$ 1.51 (s, 6H), 1.93 (m, 2H), 2.33 (t, 2H, $J$ = 6.5 Hz), 2.91 (dd, 1H, $J$ = 13.2 and 10.1 Hz), 3.23 (dd, 1H, $J$ = 13.2 and 4.1 Hz), 3.37 (t, 1H, $J$ = 6.7 Hz), 3.67 (m, 2H), 4.33 (m, 1H), 6.42 (d, 1H, $J$ = 2.1 Hz), 6.61−6.68 (3H, arene protons 6 and 3′ overlap), 6.99 (d, 2H, $J$ = 8.7 Hz), 8.42 (d, 1H, $J$ = 7.9 Hz), 8.52 (t, 1H, $J$ = 5.7 Hz). For $^1$H spectrum with structure assignment see S-15. $^{13}$C NMR (DMSO-$d_6$, 100 MHz): $\delta$ 26.73, 30.75, 30.78, 31.45, 34.52, 41.11, 41.29, 52.36, 53.10, 113.91, 114.62, 118.87, 120.29, 140.72, 141.97, 142.21, 144.76, 155.01, 170.65, 170.88, 171.03, 171.78. For $^{13}$C spectrum with structure assignment see S-16. HRMS (ESI+); calcd for $C_{25}H_{31}N_3O_9S$ $[M + H]^+$: 549.1859; found: 549.1871.

*3-Hydroxy-2-GSH-BPA*. Off-white solid; $^1$H NMR (DMSO-$d_6$, 400 MHz): $\delta$ 1.57 (s, 3H), 1.63 (s,3H), 1.91 (m, 2H), 2.30 (t, 2H, $J$ = 7.0 Hz), 2.41 (dd, 1H, $J$ = 12.0 and 10.3 Hz), 2.62 (dd, 1H, $J$ = 12.1 and 4.7 Hz), 3.40 (t, 1H, $J$ = 6.4 Hz), 3.65 (m, 2H), 4.16 (m, 1H), 6.59 (d, 2H, $J$ = 8.7 Hz), 6.76 (d, 1H, $J$ = 8.1 Hz), 6.79 (d, 2H, $J$ = 8.7 Hz), 6.86 (d, 1H, $J$ = 8.1 Hz) 8.05 (d, 1H, $J$ = 7.5 Hz), 8.52 (t, 1H, $J$ = 5.6 Hz). For $^1$H spectrum with structure assignment see S-18. $^{13}$C NMR (DMSO-$d_6$, 100 MHz): $\delta$ 26.73, 30.93, 31.44, 32.33, 35.99, 41.19, 42.81, 52.51, 53.17, 114.49, 114.67, 116.82, 120.32, 126.75, 142.07, 143.14, 143.93, 147.75, 154.46, 170.56, 170.98, 171.66. For $^{13}$C spectrum with structure assignment see S-19. HRMS (ESI+); calcd for $C_{25}H_{31}N_3O_9S$ $[M + H]^+$: 549.1859; found: 549.1870.

*3-Hydroxy-2,5-diGSH-BPA*. Off-white solid; $^1$H NMR ($D_2O$, 400 MHz): $\delta$ 1.49 (s, 3H), 1.52 (s, 3H), 2.03−2.23 (m, 6H), 3.16 (dd, 1H, $J$ = 14.5 and 8.2 Hz), 3.34 (dd, 1H, $J$ = 14.4 and 5.0 Hz), 3.72 (m, 2H), 3.86 (m, 2H), 3.95 (m, 2H), 4.03 (dd, 1H, $J$ = 8.2 and 5.9 Hz), 4.35 (dd, 1H, $J$ = 8.0 and 5.0 Hz), 6.66 (d, 2H, $J$ = 8.8 Hz), 6.95 (d, 2H, $J$ = 8.7 Hz). For $^1$H spectrum with structure assignment see S-20. $^{13}$C ($D_2O$, 100 MHz, chemical shifts calibrated with post methanol addition): 26.12, 26.16, 31.20, 31.61, 31.64, 31.94, 35.22, 35.59, 41.63, 41.72, 43.83, 5.97, 52.99, 53.41, 115.46, 118.39, 119.78, 120.38, 123.81, 128.43, 143.92, 144.07, 145.90, 147.93, 153.58, 163.37, 163.72, 172.28, 172.94, 173.38, 174.53, 174.62. For $^{13}$C spectrum with structure assignment see S-21. HRMS (ESI+); calcd for $C_{35}H_{47}N_6O_{15}S2$ $[M + H]^+$: 855.2541; found: 855.2554.

**Stopped-flow Kinetic Analysis.** A 125 $\mu$M BPAQ solution (final concentration) in 50% methanol was mixed with various concentrations of *N*-acetylcysteine (0.050, 0.10, and 0.125 M; final concentration) in 0.050 M phosphate buffer pH 6.2 and 50% methanol using a stopped-flow spectrophotometer (TgK Scientific). Concentration dependence was carried out at 5 different temperatures: 4.6 °C, 9.6 °C, 14.5 °C, and 19.4 °C. Reactions were monitored at 400 nm. Reaction traces were fit to a sum of three exponentials using KaleidaGraph (Synergy Software). GSH reactions under the same conditions with the following changes: BPAQ concentration 65 $\mu$M; GSH concentrations 40, 20, and 10 mM.

## RESULTS

**Reaction of BPAQ with NAC and NMR Analysis of Mercapturate Products.** When BPAQ is dissolved in methanol and an aqueous solution of NAC (1.3 equiv, phosphate buffer, pH 6.2) is added, rapid decolorization of the red BPAQ solution is observed. Figure 1 shows the HPLC chromatograph of the crude mixture indicating the presence of two product peaks along with trace amounts of reduced 3-hydroxyBPA (3-OHBPA). The major product (89%) was **5-NAC**, and the minor product was **2-NAC** (11%); both products are the result of 1,6-conjugate addition (see Scheme 2). Of the three possible isomers in Scheme 2, the most easily distinguished by 1-D NMR is **2-SR** since the vicinal arene

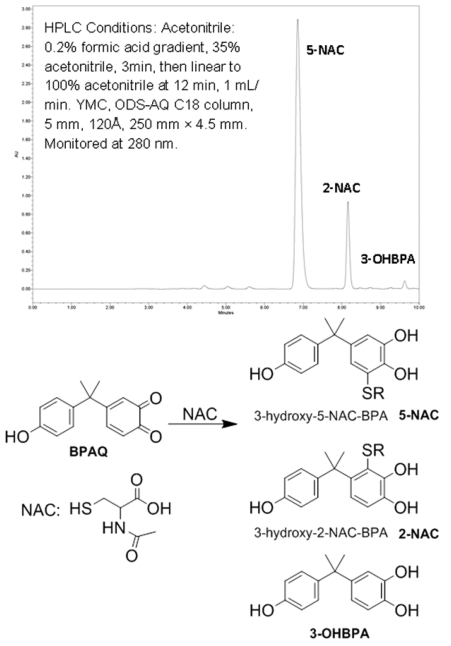


**Figure 1.** HPLC chromatograph of the reaction of BPAQ (1.0 equiv) and NAC (1.3 equiv), in $CH_3OH$:$H_2O$ 90:10, rt at 10 min.

protons H5 and H6 on the catechol ring would show a distinct coupling pattern when compared to **5-SR** or **6-SR**. Discrimination between **5-NAC** and a possible **6-NAC** isomer required a combination of both 1-D and 2-D NMR analysis. Heteronuclear (C−H) multiple bond correlation (HMBC) proved to be the most direct 2-D NMR technique in establishing the structure of **5-NAC** from **6-NAC**. HMBC optimized for three bond correlation would show three cross peaks between the quaternary, saturated carbon connecting the two arene rings to arene protons in structure **5-NAC**, while **6-NAC** would show only two correlations. Figure 2A shows the portion of the HMBC spectrum where these correlations occur, clearly showing three cross peaks consistent with isomer **5-NAC**. Several noteworthy differences in chemical shifts between the **5-NAC** and the **2-NAC** isomers were also observed. The methylene protons alpha to the sulfur atom on the NAC moiety were shifted downfield relative to NAC on the **5-NAC** adduct, while the same signals of the **2-NAC** isomer were shifted upfield relative to NAC (Figure 2B). The proton beta to the sulfur atom in the **2-NAC** isomer displayed a significant upfield shift relative to NAC, while the 5-NAC shifted upfield slightly. The **5-NAC** isomer showed significant through-space NOE correlations between arene proton H6 to both the aforementioned alpha and beta protons. These observations proved useful in establishing the structure of the larger GSH adducts (*vida infra*).

**Reaction of BPAQ with GSH and NMR Analysis of Glutathione Adducts.** When BPAQ was reacted with an aqueous solution of GSH under similar conditions used with NAC, several significant differences were observed. The chromatograph in Figure 3 shows the presence of four significant peaks when 1.3 equiv of GSH was mixed with BPAQ. The peak corresponding to 3-OHBP, the result of BPAQ reduction, is observed in much larger quantities when compared to the NAC reaction. Moreover, an early eluting peak was identified as the bis-glutathionyl adduct of BPAQ, **2,5-diGSH**. Figure 3 also shows reactions done a smaller, 0.5 mM


DOI: 10.1021/acs.chemrestox.7b00239
Chem. Res. Toxicol. XXXX, XXX, XXX−XXX

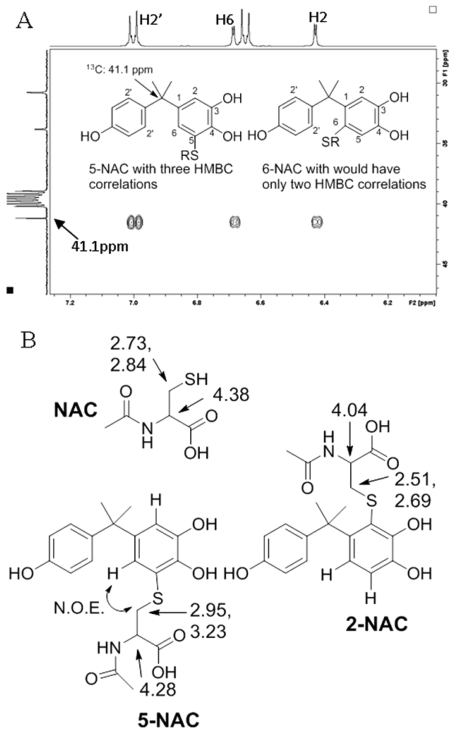


**Figure 2.** (A) Portion of the HMBC spectrum of **5-NAC** showing three cross peaks between the saturated quaternary carbon and arene protons H2, H6, and H2′. (B) Chemical shifts of the $\alpha$-methylene and $\beta$-methide protons (relative to sulfur) in **NAC**, **5-NAC**, and **2-NAC**.

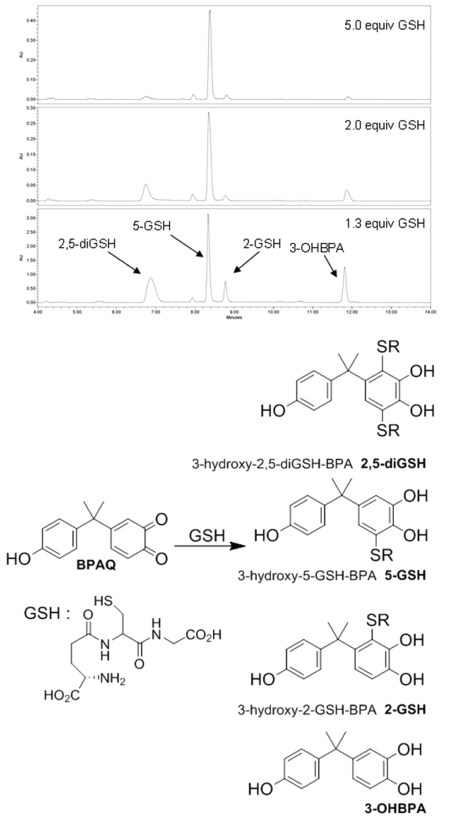


**Figure 3.** HPLC chromatographs of the reaction of BPAQ (1.0 equiv) and GSH (1.3, 2.0, and 5.0 equiv), in 50:50 $CH_3OH$:$H_2O$, 10 min at rt. HPLC conditions similar to Figure 1 except solvent gradient was 20% acetonitrile: 80% 0.2% formic acid for 2 min, then linear gradient to 100% acetonitrile at 15 min.

scale of BPAQ with increasing equivalents of GSH. At 5-fold excess of GSH, little of the **di-2,5-GSH** adduct or the reduced 3-OHBPA catechol were observed. Only monoadducted adducts were observed for NAC when using 1.3, 2.0, or 5.0 equiv of NAC. For the large-scale reaction using 1.3 equiv of GSH, isolated yields produced 17% **2,5-diGSH**, 36% **5-GSH**, 7% **2-GSH**, and 32% **3-OHBPA**.

NMR analysis of the **5-GSH** and the **2-GSH** adducts was similar to the NAC adducts. The NMR properties of the NAC adducts were useful in establishing the location of the two GSH moieties in **2,5-diGSH**; specifically, distinguishing between a 2,5-diadduct versus a 2,6- or 5,6-diadduct. First, two resolved sets of methylene protons alpha to the sulfur atom were observed: one shifted downfield and one shifted upfield relative to GSH. This is consistent with a 2,5-disubstitution profile (*vida supra*, Figure 2B). Also, through-space NOE experiments shows only one of these methylene signals correlates to the lone remaining arene proton on the catechol ring, specifically the methylene protons shifted downfield. Thus, the **2,5-diGSH** adduct is the result of two separate 1,6-conjugated additions. No products, mono- or diadducted, were the result of 1,4-addition conjugate addition.

**Kinetic Analysis of the BPAQ-NAC Reaction and BPAQ-GSH Reaction.** Using the distinct chromophore of the BPAQ, we sought to explore the kinetics of NAC and GSH conjugate addition to BPAQ by following the disappearance of BPQA at 400 nm. Figure 4A shows the decrease in the absorbance when a 125 $\mu$M solution of BPAQ in 50% methanol was mixed with various concentrations of NAC (0.050, 0.10, and 0.125 M; final concentration) in 0.050 M phosphate buffer pH 6.2 and 50% methanol using a stopped-flow spectrophotometer. To simplify the exponential decay, the reaction was made pseudo-first order using a large excess of NAC. A similar process was performed using GSH using more dilute solutions due to the reduced solubility of GSH in 50% methanol when compared to NAC. Fitting software indicates the decay is the sum of three different exponentials, indicating three separate phases. The first phase, which represents 86% of absorbance decrease, is both NAC concentration and temperature dependent. The second phase is NAC concentration independent and temperature dependent. The third phase is both temperature and NAC concentration independent, which suggests it is not part of the reaction process but an artifact of how components were mixed. Reaction with GSH displayed the same three exponential decays.

Analysis of the first phase was carried out by plotting the observed rate constants as a function of NAC or GSH concentration generating liner plots, the slope of which corresponds to the forward rate constants, $k_1$, of the bimolecular conjugate addition (Figure 4B). Nonzero intercepts indicates a reversible process, and the value of these nonzero intercept represents the reverse rate constant, $k_{-1}$. Both NAC reactions and GSH reaction displayed a reversible profile with GSH forward rate constants approximately three times faster than NAC. Each NAC concentration was carried out at four temperatures to obtain Arrhenius plots of both the forward and reverse reactions. Only three different temperatures were conducted with GSH as insolubility limited lower temperatures (Figures S3 and S4). The free energy of activation for the forward reaction was calculated at 9.2 and 7.8 kcal/mol for the NAC and GSH reactions, respectively. These $\Delta G^{\ddagger}$ values are similar to computational calculations, 10.0 kcal/mol,


DOI: 10.1021/acs.chemrestox.7b00239
*Chem. Res. Toxicol.* XXXX, XXX, XXX−XXX

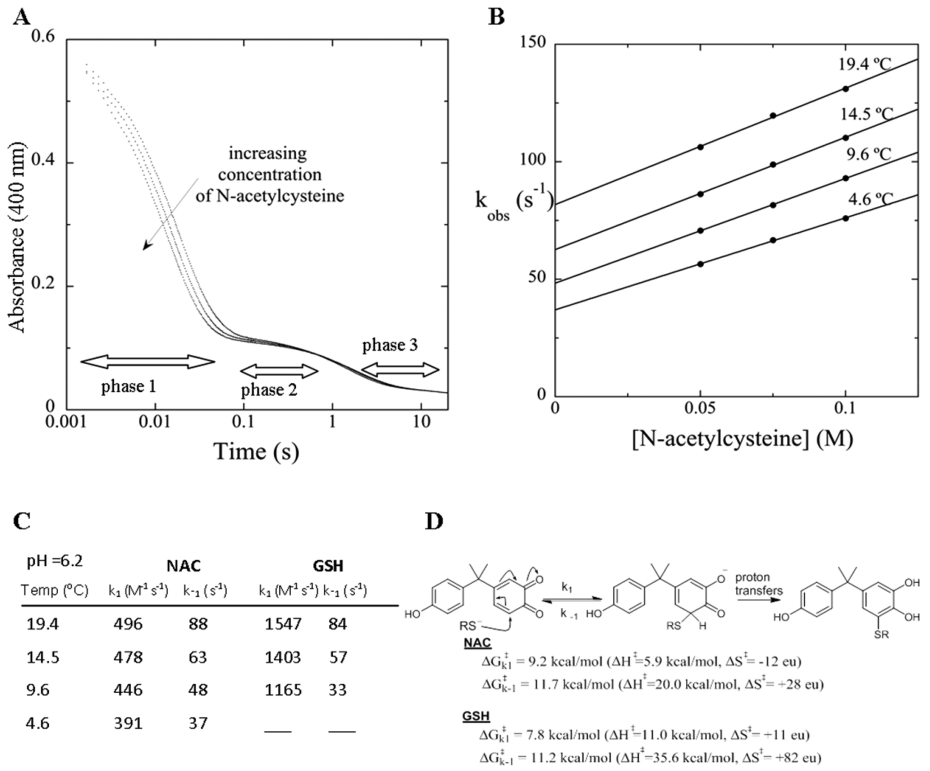


**Figure 4.** (A) The decrease in absorption of a 125 $\mu$M solution of BPAQ in 50% methanol when mixed with various, excess concentrations of NAC. (B) The observed rate constants as a function of NAC concentration run at four different temperatures. (C) Forward and reverse rate constants for the reaction BPAQ with NAC and GSH at various temperatures. (D) Free energies of activation, derived from Arrhenius plots, for both forward and reverse conjugate additions.

that model the reaction of GSH with BPAQ even though the modeled reaction assumed a 1,4-conugate addition.[24] Error analysis for the line slopes was between 4 and 6%, while the *y*-intercepts were between 7 and 10%; the final $\Delta G^{\ddagger}$ values reported are ca. ± 0.5 kcal/mol. The free energy of activation for the reverse process was similar for both NAC and GSH, 11.7 and 11.2 kcal/mol, respectively (see Figure 4C). The kinetic data of the first phase indicate a reversible 1,6-addition, which is NAC concentration dependent. The second phase observed, Figure 4A, is likely from the proton transfers involved in the tautomerization to the final catechol product. These proton transfers would be temperature dependent while independent of the concentration of NAC, which is consistent with our data.

**Discussion.** If BPAQ is a significant metabolite formed by exposure to BPA, then the most abundant biomarker would likely be mercapturates in the form of the NAC adducts.[25−27] This work provides a simple and efficient methodology in the synthesis of both the NAC and GSH adducts of BPAQ. Both nucleophiles showed exclusive preference for 1,6-addition in lieu of 1,4-addition. The formation of a bis-glutathionyl adduct with GSH as opposed to NAC, which showed no bis-*N*-acetylcysetinyl adducts, is of interest in that bis-adduct formation implies differences in the oxidation potential of GSH and NAC adducts. The mechanism for bis-adduct formation likely involves oxidation of the newly formed catechol adduct by the unreacted *o*-quinone, BPAQ (Scheme 3). This would explain the concurrent increase of 3-OHBPA observed in the GSH reaction where **2,5-diGSH** is produced as compared to the NAC reaction where very little of the 3-OHBPA catechol is observed. This also implies that the **5-GSH** adduct has a lower oxidation potential when compared to the **5-NAC** adduct. Macedo et al., using cyclic voltammetry, showed GSH adducts formed from the *o*-quinones of $\alpha$-methyldopamine and *N*-methyl-$\alpha$-dopamine had lower oxidation potentials (30 to 65 mV), when compared to the corresponding NAC adducts.[28] This suggests that GSH imparts a stronger electron-donating effect when compared to NAC increasing $k_2$ in Scheme 3, which facilitates formation of **2,5-diGSH**. If $k_1$ is greater than $k_2$, increasing GSH concentration relative to BPAQ would decrease the rate of **5-GHS-BPAQ** formation and subsequent formation of **2,5-diGSH**.

**Scheme 3. Possible Mechanism for the formation of 2,5-diGSH from Reaction of BPAQ with GSH**

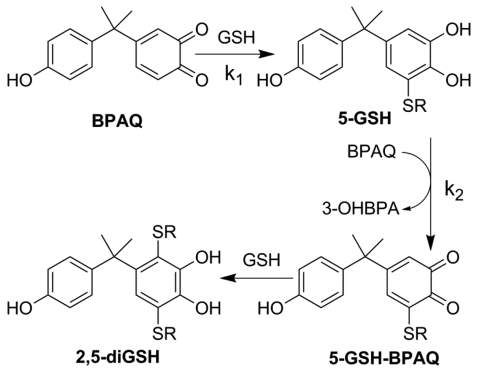


Kinetic data show the reversible nature of conjugate addition of both NAC and GSH to BPAQ. The forward rate constant for GSH reaction was significantly faster than NAC reaction. Freeman et al., also using stopped-flow analysis, observed much


DOI: 10.1021/acs.chemrestox.7b00239
Chem. Res. Toxicol. XXXX, XXX, XXX−XXX

faster conjugate addition of GSH relative to NAC with α,β-unsaturated nitro compounds derived from fatty acids and postulated this was a function of thiol acidity.[21] GSH, p$K_a$ 8.8, is more acidic than NAC, p$K_a$ 9.5.[29] Thus, at a pH of 6.2, the effective concentration of thiolate anion would be much larger with GSH solutions compared to NAC. Properties of other GSH and NAC adducts have suggested that the sulfur adduction process is reversible. GSH adducts formed between the *o*-quinone of 4-hydroxyequilenin, which exists in the oxidized *o*-quinone form, liberated 4-hydroxyequilenin and GSH when exposed to NADPH reduction.[18] Isomeric GSH adducts of the *o*-quinone formed from quercetin oxidation were shown to interconvert when allowed to equilibrate in solution.[30] GSH adducts of allyl and benzyl isothiocyanate conjugation were shown to release the isothiocyanate electrophile *in vitro*.[31] GSH conjugation is generally considered a detoxification process used to sequester reactive electrophiles such as *o*-quinones. However, GSH conjugates formed from various quinones display toxicity in certain tissues, and many of these GSH adducts stem from *p*- or *o*-quinones.[32−35] Is there a correlation between the reversible nature of quinone conjugate addition and the subsequent toxicity of GSH adducts? The BPAQ adducts synthesized in this work, efficiently made at large scale and generated from a relatively stable quinone with a distinctive chromophore, could serve as a platform for further studies to this effect.

## ■ ASSOCIATED CONTENT

### Supporting Information

The Supporting Information is available free of charge on the ACS Publications website at DOI: 10.1021/acs.chemrestox.7b00239.

Chromatography conditions for the separation of NAC and GSH adducts; 1-D and 2-D NMR spectra of NAC and GSH adducts; Arrhenius plots used to calculate free energies of activation (PDF)

## ■ AUTHOR INFORMATION


### Corresponding Author

*E-mail: dstack@unomaha.edu. Phone: 402-554-3647.

### ORCID

Douglas E. Stack: 0000-0002-8253-860X



### Funding

Partial support of the work was provided by Funds for Undergraduate Scholarly Experiences (FUSE), University of Nebraska at Omaha.


### Notes

The authors declare no competing financial interest.

## ■ ABBREVIATIONS

BPA, bisphenol A; BPAQ, bisphenol A-3,4-quinone; NAC, *N*-acetylcysteine; GSH, glutathione; IBX, 2-iodoxybenzoic acid; HMBC, heteronuclear multiple bond correlation; 3-OHBPA, 3-hydroxybisphenol A

## ■ REFERENCES


(1) Staples, C. A., Dome, P. B., Klecka, G. M., Oblock, S. T., and Harris, L. R. (1998) A review of the environmental fate, effects, and exposures of bisphenol a. *Chemosphere 36*, 2149−2173.

(2) Yoshihara, S. i., Mizutare, T., Makishima, M., Suzuki, N., Fujimoto, N., Igarashi, K., and Ohta, S. (2004) Potent estrogenic metabolites of bisphenol A and bisphenol B formed by rat liver s9 fraction: Their structures and estrogenic potency. *Toxicol. Sci. 78*, 50−59.

(3) Lee, M., Kwon, J., and Chung, M.-K. (2003) Enhanced prediction of potential rodent carcinogenicity by utilizing comet assay and apoptotic assay in combination. *Mutat. Res., Genet. Toxicol. Environ. Mutagen. 541*, 9−19.

(4) Watanabe, I., Harada, K., Matsui, T., Miyasaka, H., Okuhata, H., Tanaka, S., Nakayama, H., Kato, K., Bamba, T., and Hirata, K. (2012) Characterization of bisphenol A metabolites produced by portulaca oleracea cv. By liquid chromatography coupled with tandem mass spectrometry. *Biosci., Biotechnol., Biochem. 76*, 1015−1017.

(5) Tayama, S., Nakagawa, Y., and Tayama, K. (2008) Genotoxic effects of environmental estrogen-like compounds in cho-k1 cells. *Mutat. Res., Genet. Toxicol. Environ. Mutagen. 649*, 114−125.

(6) Naik, P., and Vijayalaxmi, K. K. (2009) Cytogenetic evaluation for genotoxicity of bisphenol-A in bone marrow cells of swiss albino mice. *Mutat. Res., Genet. Toxicol. Environ. Mutagen. 676*, 106−112.

(7) Knaak, J. B., and Sullivan, L. J. (1966) Metabolism of bisphenol A in the rat. *Toxicol. Appl. Pharmacol. 8*, 175−184.

(8) Edmonds, J. S., Nomachi, M., Terasaki, M., Morita, M., Skelton, B. W., and White, A. H. (2004) The reaction of bisphenol A 3,4-quinone with DNA. *Biochem. Biophys. Res. Commun. 319*, 556−561.

(9) Qiu, S.-X., Yang, R. Z., and Gross, M. L. (2004) Synthesis and liquid chromatography/tandem mass spectrometric characterization of the adducts of bisphenol A o-quinone with glutathione and nucleotide monophosphates. *Chem. Res. Toxicol. 17*, 1038−1046.

(10) Atkinson, A., and Roy, D. (1995) In vitro conversion of environmental estrogenic chemical bisphenol A to DNA binding metabolite(s). *Biochem. Biophys. Res. Commun. 210*, 424−433.

(11) Atkinson, A., and Roy, D. (1995) In vivo DNA adduct formation by bisphenol A. *Environ. Mol. Mutagen. 26*, 60−66.

(12) Stack, D. E., Byun, J., Gross, M. L., Rogan, E. G., and Cavalieri, E. L. (1996) Molecular characteristics of catechol estrogen quinones in reactions with deoxyribonucleosides. *Chem. Res. Toxicol. 9*, 851−859.

(13) Wu, Q., Fang, J., Li, S., Wei, J., Yang, Z., Zhao, H., Zhao, C., and Cai, Z. (2017) Interaction of bisphenol A 3,4-quinone metabolite with glutathione and ribonucleosides/deoxyribonucleosides in vitro. *J. Hazard. Mater. 323*, 195−202.

(14) Bolton, J. L., Acay, N. M., and Vukomanovic, V. (1994) Evidence that 4-allyl-o-quinones spontaneously rearrange to their more electrophilic quinone methides: Potential bioactivation mechanism for the hepatocarcinogen safrole. *Chem. Res. Toxicol. 7*, 443−450.

(15) Iverson, S. L., Hu, L. Q., Vukomanovic, V., and Bolton, J. L. (1995) The influence of the p-alkyl substituent on the isomerization of o-quinones to p-quinone methides: Potential bioactivation mechanism for catechols. *Chem. Res. Toxicol. 8*, 537−544.

(16) Stack, D. E., and Mahmud, B. (2017) Efficient access to bisphenol a metabolites: A one-pot synthesis of the monocatechol, mono-o-quinone, dicatechol, and di-o-quinone of bisphenol A. *Synth. Commun.*, 1.

(17) Chandrasena, R. E. P., Edirisinghe, P. D., Bolton, J. L., and Thatcher, G. R. J. (2008) Problematic detoxification of estrogen quinones by nad(p)h-dependent quinone oxidoreductase and glutathione-s-transferase. *Chem. Res. Toxicol. 21*, 1324−1329.

(18) Peng, K.-W., Chang, M., Wang, Y.-T., Wang, Z., Qin, Z., Bolton, J. L., and Thatcher, G. R. J. (2010) Unexpected hormonal activity of a catechol equine estrogen metabolite reveals reversible glutathione conjugation. *Chem. Res. Toxicol. 23*, 1374−1383.

(19) Awad, H. M., Boersma, M. G., Boeren, S., van Bladeren, P. J., Vervoort, J., and Rietjens, I. M. C. M. (2003) Quenching of quercetin quinone/quinone methides by different thiolate scavengers: Stability and reversibility of conjugate formation. *Chem. Res. Toxicol. 16*, 822−831.

(20) Murty, V. S., and Penning, T. M. (1992) Polycyclic aromatic hydrocarbon (pah) ortho-quinone conjugate chemistry: Kinetics of thiol addition to pah ortho-quinones and structures of thioether adducts of naphthalene-1,2-dione. *Chem.-Biol. Interact. 84*, 169−188.

(21) Baker, L. M. S., Baker, P. R. S., Golin-Bisello, F., Schopfer, F. J., Fink, M., Woodcock, S. R., Branchaud, B. P., Radi, R., and Freeman, B.




DOI: 10.1021/acs.chemrestox.7b00239
*Chem. Res. Toxicol.* XXXX, XXX, XXX−XXX

A. (2007) Nitro-fatty acid reaction with glutathione and cysteine: Kinetic analysis of thiol alkylation by a michael addition reaction. *J. Biol. Chem. 282*, 31085−31093.
(22) Chen, J., Jiang, X., Carroll, S. L., Huang, J., and Wang, J. (2015) Theoretical and experimental investigation of thermodynamics and kinetics of thiol-michael addition reactions: A case study of reversible fluorescent probes for glutathione imaging in single cells. *Org. Lett. 17*, 5978−5981.
(23) Frigerio, M., Santagostino, M., and Sputore, S. (1999) A user-friendly entry to 2-iodoxybenzoic acid (IBX). *J. Org. Chem. 64*, 4537−4538.
(24) Kolšek, K., Sollner Dolenc, M., and Mavri, J. (2013) Computational study of the reactivity of bisphenol A-3,4-quinone with deoxyadenosine and glutathione. *Chem. Res. Toxicol. 26*, 106−111.
(25) Van Welie, R. T. H., Van Dijck, R. G. J. M., Vermeulen, N. P. E., and Van Sittert, N. J. (1992) Mercapturic acids, protein adducts, and DNA adducts as biomarkers of electrophilic chemicals. *Crit. Rev. Toxicol. 22*, 271−306.
(26) De Rooij, B. M., Commandeur, J. N. M., and Vermeulen, N. P. E. (1998) Mercapturic acids as biomarkers of exposure to electrophilic chemicals: Applications to environmental and industrial chemicals. *Biomarkers 3*, 239−303.
(27) Mathias, P. I., and B'Hymer, C. (2016) Mercapturic acids: Recent advances in their determination by liquid chromatography/mass spectrometry and their use in toxicant metabolism studies and in occupational and environmental exposure studies. *Biomarkers 21*, 293−315.
(28) Macedo, C., Branco, P. S., Ferreira, L. M., Lobo, A. M., Capela, J. P., Fernandes, E., Bastos, M. d. L., and Carvalho, F. (2007) Synthesis and cyclic voltammetry studies of 3,4-methylenedioxymethamphetamine (MDMA) human metabolites. *J. Health Sci. 53*, 31−42.
(29) Trujillo, M., and Radi, R. (2002) Peroxynitrite reaction with the reduced and the oxidized forms of lipoic acid: New insights into the reaction of peroxynitrite with thiols. *Arch. Biochem. Biophys. 397*, 91−98.
(30) Boersma, M. G., Vervoort, J., Szymusiak, H., Lemanska, K., Tyrakowska, B., Cenas, N., Segura-Aguilar, J., and Rietjens, I. M. C. M. (2000) Regioselectivity and reversibility of the glutathione conjugation of quercetin quinone methide. *Chem. Res. Toxicol. 13*, 185−191.
(31) Bruggeman, I. M., Temmink, J. H. M., and Van Bladeren, P. J. (1986) Glutathione- and cysteine-mediated cytotoxicity of allyl and benzyl isothiocyanate. *Toxicol. Appl. Pharmacol. 83*, 349−359.
(32) Monks, T. J., and Lau, S. S. (1997) Biological reactivity of polyphenolic-glutathione conjugates. *Chem. Res. Toxicol. 10*, 1296−1313.
(33) Monks, T. J., Anders, M. W., Dekant, W., Stevens, J. L., Lau, S. S., and Van Bladeren, P. J. (1990) Glutathione conjugate mediated toxicities. *Toxicol. Appl. Pharmacol. 106*, 1−19.
(34) Lau, S. S., Jones, T. W., Highet, R. J., Hill, B. A., and Monks, T. J. (1990) Differences in the localization and extent of the renal proximal tubular necrosis caused by mercapturic acid and glutathione conjugates of 1,4-naphthoquinone and menadione. *Toxicol. Appl. Pharmacol. 104*, 334−350.
(35) Lau, S. S., Hill, B. A., Highet, R. J., and Monks, T. J. (1988) Sequential oxidation and glutathione addition to 1,4-benzoquinone: Correlation of toxicity with increased glutathione substitution. *Mol. Pharmacol. 34*, 829−836.


DOI: 10.1021/acs.chemrestox.7b00239
*Chem. Res. Toxicol.* XXXX, XXX, XXX−XXX